

high demand and therefore improve the overall profit. However, whether higher revenues can be achieved with flexible CO₂ capture will depend on the electricity market and its price patterns. Van der Wijk et al.⁹ suggested that the main benefit of flexible carbon capture is that it provides the plant operator with increased capacity reserve. Brunnemann et al.¹⁰ demonstrated that steam used for solvent regeneration in the capture unit can be rather promptly throttled and expanded in the low pressure steam turbine to generate balancing energy. The study focuses more on the configuration of power plant cycle, and thus, a more detailed investigation of the dynamics of the capture systems is necessary.

In case of complex processes and power plants, dynamic simulation and optimization are the state of the art approaches for the evaluation of control strategies and achievable performance.¹¹ An increasing number of publications documents studies on transient performance of PCC plants by means of dynamic simulations, whereby in most cases the dynamic model was validated by comparison with steady-state experimental data.^{12–16} Validation against measurements obtained during transient operation, which is important to verify the validity and to improve the accuracy of the dynamic model, is documented in few publications. Kvamsdal et al.¹⁴ described the validation of an absorber model by comparison with transient experimental data obtained at a pilot-scale absorber owned by the NTNU and the SINTEF laboratory. Moreover, they presented a comparison of different parameter correlations for the reaction rate constant and concluded that the results obtained from the validation of one specific pilot plant are not necessarily applicable to plants of different size and operated under different conditions. Posch et al.¹⁷ presented the comparison of test run data and simulation results for the dynamic operation of an absorber column whereby both the inlet temperature of the solvent and the flue gas were increased. From a second simulation case, in which the flue gas flow was increased, it was concluded that nonoptimized PID controller settings can lead to oscillations in some process variables and to a drop of the separation efficiency below 90% during the transient. Both these studies were limited to the modeling and simulation of the absorber column, while the dynamics of CO₂ capture plants was determined by the complex interaction between the absorber and the stripper column. Åkesson et al.¹⁸ developed a detailed dynamic model of the complete capture plant. Simulation results were compared against transient data obtained from open-loop experiments at the Esbjerg pilot plant in Denmark.¹⁹ Furthermore, the detailed model was reduced to be able to solve optimal control problems. It was thus demonstrated that the reduced model was sufficiently accurate for the purpose of dynamic optimization.

Enaasen Flø et al.²⁰ adapted the absorber model developed by Kvamsdal et al.¹⁴ and extended it by including models of the remaining capture plant components. System model validation against two dynamic data sets generated at a pilot plant was presented. It was concluded that step changes in solvent flow rate cause greater process disturbances than changes in reboiler duty. Online density measurements and solvent samples were used to monitor changes in CO₂ loading during the experiment.

Bilyok et al.²¹ presented a comprehensive validation of a capture plant model using transient data from a pilot plant at the University of Texas. Experiments involving step-like changes of a selected variable were not possible; therefore, data related to significant transients of the plant input were

chosen to ensure that the change in other variables was minimal. In three validation cases, satisfactory agreement between model predictions and measurements was demonstrated. The validated model was used to perform two case studies, and it was concluded that the flue gas moisture content is an important parameter for model validation.

Walters et al.²² developed a simplified model and compared its results to a complex Aspen Plus model as well as dynamic pilot plant data. The low-order lumped parameter model used rate-based mass transfer and semiempirical thermodynamics. It was concluded that the model is capable of predicting the plant performance especially near the design point and is suitable for control studies in future work.

These studies demonstrated that dynamic model validation is essential to ensure that the developed model predicts transient operation with sufficient accuracy for control design. One of the main purposes of capture plant models is the study of the impact of transient operation on the plant and CO₂ capture performance in realistic situations.

The general aim of this paper is to further broaden the knowledge base in the field of dynamic modeling and validation of PCC systems by considering new flexible operation scenarios. Therefore, this paper presents the dynamic validation of an amine-based PCC plant model, which was developed using the open source ThermalSeparation Modelica library.^{23,24} The transient experimental measurements were obtained during step-response tests at the capture pilot plant built at the Maasvlakte power station in the Netherlands.²⁵ Moreover, the validated model was used to investigate a dynamic operating scenario, whereby the steam supply from the power plant to the capture unit was promptly decreased to quickly respond to fluctuations in the electricity demand. The aspect of CO₂ storage is not considered in this study.

The subject matter is organized as follows. Section 2 provides a brief description of the PCC process and of the pilot plant configuration. Section 3 illustrates the modeling approach together with the utilized model libraries. Section 4 describes the PCC plant model, the transient experiments, and subsequently the dynamic model validation. Section 5 discusses the case study, while Section 6 presents concluding remarks.

2. POSTCOMBUSTION CAPTURE PROCESS

2.1. General Process Description. Figure 1 visualizes a typical process scheme of a PCC plant based on chemical

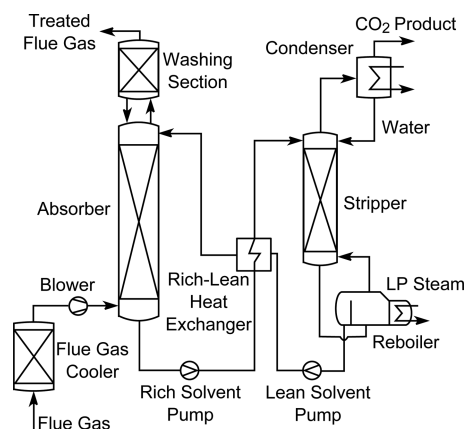


Figure 1. Simplified process flow diagram of a typical postcombustion CO₂ capture plant.

absorption, with the absorber and stripper column as the main process units. The flue gas from the power plant, which contains about 12–15 mol % CO₂, is first cooled to temperatures in the range of 35–40 °C and then sent to the bottom of the absorber column. In the absorber, CO₂ is removed from the flue gas by means of reactive absorption into the amine-based solvent. The treated flue gas exits the absorber at the top and passes through the washing section. The washing section is used to maintain the water balance of the capture system and to prevent solvent loss. To this end, the temperature of the washing section is controlled. Maintaining the water balance is important for keeping the solvent concentration constant. Thereafter, the treated flue gas containing about 1–2 mol % CO₂ is released to the environment. This corresponds to a target capture rate of 90%.

The rich solvent at the bottom of the absorber is routed to the top of the stripper column after it passes the rich/lean heat exchanger for recovery of thermal energy from the lean solvent stream. In the stripper, the rich solvent is regenerated at around 120 °C. The required energy is supplied by steam, which is extracted at the crossover pipe between the intermediate and low pressure steam turbine of the power plant. The solvent regeneration is therefore primarily responsible for the efficiency penalty on the energy conversion efficiency of the power plant. The regenerated solvent from the bottom of the stripper is recycled to the top of the absorber. The resulting CO₂ product, with a purity typically above 99 mol %, is released from the condenser, in which water and solvent are condensed and returned to the stripper. Thereafter, CO₂ can be compressed and transported to its permanent storage location in deep geological formations. The CO₂ compression process is, in addition to solvent regeneration process, the largest energy demand within the entire CO₂ capture plant.

2.2. Pilot Plant Configuration. As part of the national R&D program on CCS of the Netherlands (CATO-2), the research institute TNO has commissioned in 2008 a PCC pilot plant located at the site of the coal-fired Maasvlakte power station in Rotterdam,²⁵ see Figure 2. The capture plant can process up to 1500 Nm³/h of flue gas from the adjacent power plant, which corresponds to 0.3 MW_{el} power output. Recent modifications to the pilot plant resulted however in an increase of the pressure drop of the absorber section. Because of limitations of the blower capacity, the maximum flue gas flow



Figure 2. TNO CO₂ capture pilot plant at the Maasvlakte power plant in the Netherlands.

that can currently be processed reduced to 800 Nm³/h. The nominal operating conditions of the capture plant are summarized in Table 1. The pilot plant is designed for testing

Table 1. Nominal Operating Conditions of the Maasvlakte Pilot-Scale Capture Plant

variable	unit	value
flue gas flow	[Nm ³ /h]	800
flue gas CO ₂ concentration (dry)	[mol %]	14.4
flue gas absorber inlet temperature	[°C]	40
solvent flow	[ton/h]	3.2
total solvent hold-up	[m ³]	2.5
solvent hold-up time	[min]	52
lean solution temperature	[°C]	40
MEA concentration	[wt %]	30
stripper pressure	[bar]	1.9
CO ₂ product temperature	[°C]	25
CO ₂ product concentration	[mol %]	98.3
CO ₂ capture rate	[%]	95

of different solvents. During the campaign corresponding to the measurements presented in this paper, the solvent monoethanolamine (MEA) was used. MEA is considered as a baseline solvent due to its high reaction rate with CO₂, its low costs, and the long lasting experience with natural gas sweetening.^{2,3} The thermal energy required by solvent regeneration is however relatively high compared to novel solvents such as blends with secondary and tertiary amines, polyamines, and alkali salts.^{26,27} Furthermore, MEA starts to degrade at temperatures above 120 °C. Therefore, the reboiler temperature is controlled at 120 °C by adjusting the steam flow to the reboiler. The steam is supplied by an electrical steam generator. In the pilot plant, a 30 wt % MEA solution is employed. Higher concentrations of MEA lead to a higher degradation rate and to elevated reboiler temperatures, which would consequently also result in a higher degradation rate.²⁸ The stripper pressure is controlled with a valve downstream of the stripper condenser. The water balance in the pilot plant can be manually checked via the level in the stripper sump, which is not controlled. For example, a surplus in water leads to an increasing level in the stripper sump. Figure 3 provides a process flow diagram of the pilot plant including the control structure, while Table 2 shows a list of controlled and corresponding manipulated variables.

3. MODELS

The dynamic model of the capture plant is implemented in a computer code using the Modelica modeling language²³ because of its many positive characteristics. Modelica is acausal, declarative, and object-oriented, and it is especially suited to component-oriented multidomain modeling of complex systems. Modelica is a nonproprietary modeling language and is supported by various proprietary as well as open source simulation tools.

Two different libraries were used for the development of the system model of the CO₂ capture unit. The component models for the separation columns, the reboiler, the condenser, the column sumps, and the media packages were reused from the ThermalSeparation library.²⁴ Other models for heat exchangers as well as pumps and valves were taken from the ThermoPower library.^{29,30} The purpose of the ThermalSeparation library is the dynamic simulation of general thermal separation processes. So

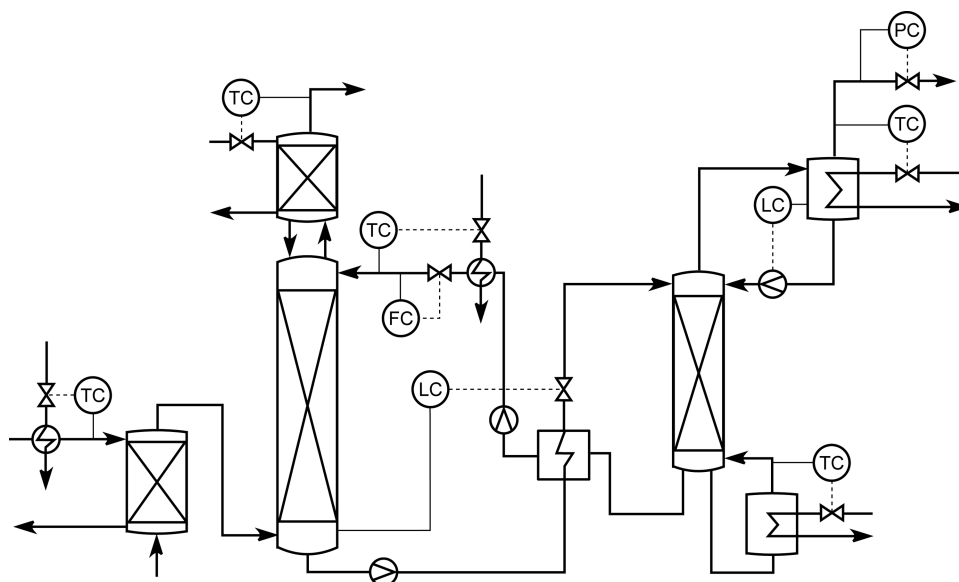


Figure 3. Process flow diagram of pilot plant including the control structure.

Table 2. Controlled and Manipulated Variables of the Capture Pilot Plant

controlled variable	manipulated variable
flue gas flow	flue gas valve opening
lean solvent flow	lean solvent valve opening
absorber sump level	rich solvent valve opening
lean solvent temperature	lean solvent cooling water valve opening
caustic solution temperature	caustic solution cooling water valve opening
clean gas temperature	wash water cooling water valve opening
stripper pressure	CO ₂ product valve opening
reboiler temperature	steam valve opening
stripper condenser level	stripper condensate pump speed

far, the library implements models for absorption and rectification columns. Furthermore, models for different column types such as tray columns, spray columns, and structured and random packed columns are also available.

The column model is developed following a modeling approach that allows the flexible adaptability of models, and it comprises of several replaceable models and packages that allow the user to change, for example, working fluid models or pressure loss correlations to meet individual modeling requirements. An important feature of the column model is the possibility to exchange the balance equations allowing the modeler to opt between a rate-based or an equilibrium-based formulation of the heat and mass transfer across the phase boundary. A more detailed description of the balance and constitutive equations that are used within the column model is given by Dietl et al.^{24,31} The model can be discretized in the axial direction, and perfect mixing of the liquid and vapor bulk phase is assumed for each stage. The modeler can specify inert components that will not cross the phase boundary. If chemical reactions shall be considered, then they are accounted for in the liquid phase. The reactions can be implemented in an equilibrium or kinetically controlled fashion, independent from the chosen model for the balance equations and the selected film model. The film model contains the calculation of the thermodynamic equilibrium. Ongoing work and future developments are intended to broaden the scope of application of the ThermalSeparation library toward different process types

such as, for example, extraction or adsorption. Moreover, activities focus also on interfacing external fluid property libraries to allow the easy use of a wide range of process fluids.^{32,33}

The ThermoPower library contains reusable components for the modeling of thermohydraulic processes and power plants using working fluid models that are suitable to describe water or ideal gases. The components can be used for system-level modeling and simulation to study, for example, control system design of energy conversion systems. The ThermoPower component models needed for the modeling of the capture plant were adapted to allow for the use of other working fluid models from the ThermalSeparation library.

The main phenomena that are involved in reactive absorption of CO₂ from flue gas into a MEA solution are mass and heat transfer between the vapor and liquid phase in the column and chemical reactions between the solvent and CO₂. These phenomena can be modeled with different level of complexity.³⁴ A simple representation of the mass and heat transfer assumes thermodynamic equilibrium between the liquid and vapor phase at each theoretical column stage. A more rigorous and accurate formulation accounts for mass and heat transfer limitations and is therefore based on rate equations. In both approaches, chemical equilibrium or detailed reaction kinetics can be assumed. A rate-based model considering reaction kinetics allows researchers to obtain the most accurate performance predictions, but it leads to high model complexity and high computational cost.

The model of the postcombustion CO₂ capture unit is intended for integration into a model of the entire power plant. Ultimately, its purpose is to study the interaction of different plant units during transient operations. In the instance of a plant-wide system analysis, a reduction in the degree of detail would be required to improve the model robustness and to allow for reasonable simulation time. In terms of accuracy of model predictions, it is worth mentioning that deviations in the absolute values of process variables have often a negligible impact on the predictions of system dynamics, which are of main interest in this type of studies. For this reason, the equilibrium-based approach assuming thermodynamic and

Table 3. Coefficients for Calculation of Thermodynamic Equilibrium and Heat of Reaction, As Used in Eqs 1 and 2

c_0	c_1	c_2	c_3	c_4	c_5	c_6	c_7	c_8
22.53	-7904	105	-16 810	-286.4	26 480	381.7	8295	-257.4

chemical equilibrium at each column stage was adopted for the modeling of the absorber and stripper component. The implementation is based on the method described by Oexmann,²⁶ in which the chemical reaction, the thermodynamic equilibrium, and the diffusive resistance are combined in one expression. This expression also accounts for the mass transfer that occurs due to the chemical reaction by adjusting the thermodynamic equilibrium without modeling the reaction kinetics in detail.

It is assumed that CO₂ that crosses the phase boundary reacts instantaneously with the solvent. This approach has the advantage that only the equations for the thermodynamic equilibrium, given as

$$\ln p_{\text{CO}_2}^* = c_0 + c_1 \frac{1}{T} + c_2 \alpha + c_3 \frac{\alpha}{T} + c_4 \alpha^2 + c_5 \frac{\alpha^2}{T} + c_6 \alpha^3 + c_7 \frac{\alpha^3}{T} + c_8 \alpha^4 \quad (1)$$

and for the heat of reaction, written as

$$\Delta h_{\text{CO}_2} = -R(c_1 + c_3 \alpha + c_5 \alpha^2 + c_7 \alpha^3) \quad (2)$$

must be implemented. A rather complicated implementation of the chemical reaction including several side reactions, for which actual kinetic data is very scarce, can be avoided.

The partial pressure of CO₂ is denoted by $p_{\text{CO}_2}^*$, α is the CO₂ loading of the liquid medium at the temperature T , R is the ideal gas constant, and Δh_{CO_2} is the combined absorption and reaction enthalpy of CO₂. The coefficients c_0 to c_8 are given in Table 3. They were determined by Oexmann by fitting of measurement data published by Jou et al.,³⁵ Hilliard,²⁷ and Dugas.³⁶

The equilibrium model of the column contains a calibration factor c , which can be tuned, for example, to improve the agreement between model predictions and experimental measurements. The calibration factor is described by

$$K = c \times \frac{p_{\text{CO}_2}^*}{p} \quad (3)$$

and directly influences the equilibrium constant K , which is calculated based on the partial pressure of CO₂ and the absolute column pressure p .

Additionally, the following general assumption are made.

- Constituents of the absorber gaseous medium, the flue gas, are CO₂, H₂O, N₂, and O₂. The latter two substances are considered inert in the gas phase.
- Constituents of the stripper gaseous medium are CO₂ and H₂O.
- Constituents of the liquid medium are CO₂, H₂O, and MEA. MEA is considered to be nonvolatile.
- The gas phase is assumed as ideal gas.
- The liquid density and the heat capacity of the aqueous MEA solution can be described using empirical correlations developed by Oexmann.²⁶
- The components are well insulated; hence, heat transfer of the components to the surrounding can be neglected.

- Column pressure drop and liquid hold-up can be calculated using the correlations developed by Stichlmair.³⁷
- No reactions take place in components other than the absorber and stripper column.
- The volume of the pipes is small compared to the sumps and can therefore be neglected.
- Heat transfer coefficients in the heat exchangers are constant.
- Heat transfer in the condenser and reboiler is assumed to be fast, and therefore, the heat transfer is modeled by directly providing the heat duty as an input to the condenser and reboiler model.
- Control of the flue gas flow and the stripper pressure is assumed to be fast, and therefore, both variables are used as direct input to the model.

On the basis of these assumptions, the system model of the capture plant was developed using suitable component/subcomponent models of the ThermalSeparation and ThermoPower libraries. A scheme of the capture plant model is shown in Figure 4. In Table 4, the model parameters are summarized,

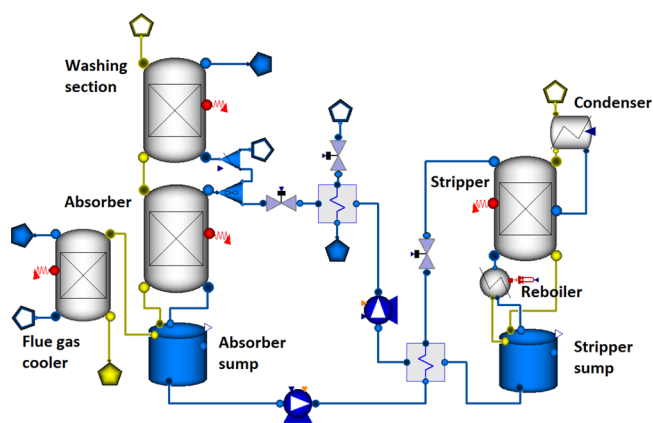


Figure 4. Object diagram of the dynamic model of the capture pilot plant.

and in Table 5, an overview of the model input variables is given. These values are based on pilot plant measurements. The number of equilibrium stages has been determined with the help of detailed standalone absorber and stripper models. They have been tuned such that the overall column performance at nominal operating conditions matched the simulation results of a validated steady-state model. A more detailed description of the model development and the individual components is given by van de Haar.³⁸

4. EXPERIMENTS

Step response tests were performed to study the dynamics of the CO₂ capture pilot plant and to obtain data for model validation. The main process variables that are expected to undergo frequent time-variations during normal operation are the flue gas flow rate, due to load variations in the power plant, and the solvent flow rate, which is typically adjusted to maintain a constant liquid-to-gas (L/G) ratio in the absorber, which

Table 4. Model Parameters of the Main Pilot Plant Components

column parameters	unit	absorber	stripper	FG cooler	washing section
packed height	[m]	8.4	8.2	2.0	2.0
column diameter	[m]	0.65	0.45	0.65	0.65
no. of equilibrium stages		20	5	5	5
packing type		IMTP 50	IMTP 50	IMTP 50	Mellapak 250Y
- void fraction		0.98	0.98	0.98	0.98
- specific surface area	[m ² /m ³]	102	102	102	256
- heat capacity	[J/(kg K)]	460	460	460	460
- density	[kg/m ³]	7900	7900	7900	7900
sump volume	[m ³]	1270	770		
solvent residence time	[min]	28	17		
calibration factor <i>c</i>		1.117	1.0		
heat exchanger parameters		unit	rich-lean HEX	lean solvent cooler	
overall heat transfer coefficient		[W/m ² K]	1400	1500	
area		[m ²]	29.5	10.0	

Table 5. Input Variables to the Pilot Plant Model

input variable	unit	value
flue gas inlet temperature	[°C]	50
flue gas inlet composition (<i>x</i> _{H₂O} , <i>x</i> _{O₂} , <i>x</i> _{CO₂} , <i>x</i> _{N₂})	[mol/mol]	0.074, 0.054, 0.133, 0.739
flue gas cooler water temperature	[°C]	40
flue gas cooler water flow	[L/min]	54
washing water flow	[L/min]	50
absorber outlet pressure	[bar]	1.013
cooling water temperature	[°C]	19
stripper outlet pressure	[bar]	1.90

results in an approximately constant capture rate. Changes were therefore applied separately to the flue gas and to the solvent flow rate, while the set points of the controllers of all other process variables are kept constant. These are, for example, the reboiler temperature, the stripper pressure, and the lean solvent temperature. To perform prompt perturbations, both flow controllers were operated in manual mode. If the control is in open-loop, the controller has no influence on the system response, which allows researchers to monitor the response of the process rather than the response of the control loop.

The set points for the transient tests are summarized in Table 6. Starting from nominal operating conditions, first the

Table 6. Process Conditions of the Step Response Tests^a

	solvent flow [ton/h]	flue gas flow [Nm ³ /h]	L/G ratio [kg/Nm ³]
nominal operation	3.2	800	4.0
test A1	3.2	580	5.5
test A2	3.2	800	4.0
test B1 ^b	4.4	800	5.5

^aPerturbed variable is highlighted in bold. ^bBecause of failure of the lean solvent control valve during this test, only the first 30 min of the measured data after the perturbation are usable.

flue gas flow rate was decreased stepwise (test A1) and subsequently increased (test A2) returning to the initial operating point. Finally, the solvent flow rate was perturbed by an upward step in the same manner (test B1). Each perturbation was applied after the system reached steady-state operation, which typically required 2 h. The height of the steps

was chosen such that a clear system response can be observed without exceeding the plant capacity.

In addition to temperature, pressure, and mass flow measurements, samples of the lean and rich solvent were taken at the sump of the absorber and the stripper to allow for comprehensive comparison of measurements and model predictions. As the largest changes in solvent composition occur directly after a perturbation, samples were taken every 10 min during the first half hour after the step change, and thereafter at 60 as well as 120 min. The CO₂ loading and the molarity of MEA were determined by means of solvent sample analysis. The uncertainty of the used measurement method was about 5% and indicated with error bars in the plots comparing the experimental data and simulation results, see Figure 5d and 7d. Refer to the Supporting Information of this paper for tabulated data of the described experiments.

4.1. Validation. The aim of the test runs was to obtain measurement data for quantitative validation of the dynamic model. The validation shall demonstrate if process transients can be predicted with accuracy sufficient for control design using an equilibrium-based model for reactive absorption of CO₂.

In a first step, data reconciliation was performed to minimize deviations between measured and simulated values for the model output variables rich loading, lean loading, and CO₂ capture rate by adjusting model input variables, namely flue gas flow, reboiler temperature, and absorber calibration factor. Additionally, the heat transfer coefficients of the heat exchanger components were fitted to steady-state experimental data at nominal operating condition.

Tuning the calibration factor, see eq 3, allows researchers to account for deviations between measurements and model predictions, which are in particular related to the modeling assumption regarding the mass and heat transfer (equilibrium-based), and the chemical reaction (chemical equilibrium). The loading of the rich solvent exiting the absorber bottom is the most sensitive variable with respect to the calibration factor and was therefore selected as model output variable.

The calibration factor of the stripper was not adjusted during data reconciliation because ad hoc investigation demonstrated that the stripper column can be accurately modeled by assuming ideal equilibrium conditions. Furthermore, the lean loading was selected as output variable because initially the model significantly overestimated the lean loading, which indicated that a higher heat duty would be required to

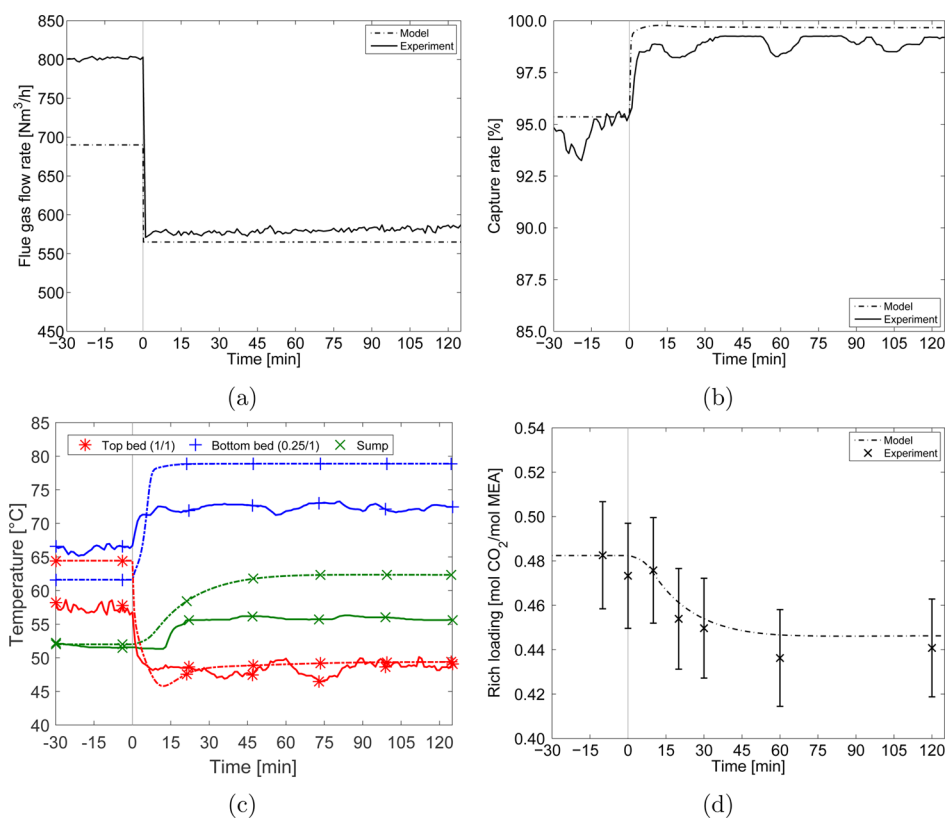


Figure 5. Comparison of experimental data (solid line) and model results (dashed line) for open-loop step response test: decrease in flue gas flow rate. (a) Flue gas flow rate, (b) capture rate, (c) absorber column temperatures, and (d) rich solvent loading.

Table 7. Comparison of Steady-State Model Results for the Case of Unfitted and Fitted Model Parameters with Capture Pilot Plant Measurements

		measurements (on-design)	model results (on-design)	measurements (off-design)	model results (off-design)
flue gas flow rate	[Nm ³ /h]	800	690	582	565
lean solvent flow rate	[t/h]	3.2	3.2	3.2	3.2
L/G ratio	[kg/kg]	3.0	3.5	4.1	4.2
stripper pressure	[bar]	1.90	1.90	1.90	1.90
reboiler temperature	[°C]	120	121.3	120	121.3
capture rate	[%]	95.2	95.3	98.8	99.7
rich loading	[mol/mol]	0.483	0.482	0.437	0.446
lean loading	[mol/mol]	0.236	0.232	0.229	0.232
absorber calibration factor			1.118		1.118
stripper calibration factor			1.0		1.0

regenerate the solvent. Unfortunately, not enough measurements were available to reproduce the energy balance of the reboiler. To correct the mismatch in lean loading, the reboiler temperature, which is imposed as an input variable of the model, was adjusted during the data reconciliation (see Table 7).

During the experiments, leakage of the flue gas flow downstream the flow rate measurement device was observed, and therefore, the recorded flow measurements were affected. The flue gas flow measurements were therefore corrected to obtain a good agreement between the measured and predicted CO₂ capture rate. (The capture rate is defined as the amount of CO₂ captured in the absorber in relation to the total amount of CO₂ entering the absorber column. Here, the capture rate was calculated based on the measured CO₂ concentration at the inlet and outlet of the absorber under the assumption that the purity of the captured CO₂ is approximately 1.) At on-design

operation, the leakage flow turned out to be much larger (110 Nm³/h) than that at off-design operation (17 Nm³/h). Unfortunately, also the measurements of the gaseous flow at the absorber and stripper top displayed errors due to instrument malfunction and thus could not be used as redundant measurements to confirm the leakage flow. Table 7 summarizes the results of the parameter fitting and variable adjustments.

The process variables used for the quantitative comparison of experimental data and model predictions were the capture rate, the absorber temperature profile, and the rich and lean solvent loading. These variables were chosen because they are largely affected by the applied changes in flue gas or solvent flow rate.

In the following, the model validation is illustrated based on the data acquired during test A1, step decrease in the flue gas flow rate, and test A2, inverse step increase in flue gas flow rate.

The comparison of simulation results and measurements for test A1 are shown in Figures 5 and 6. The stepwise decrease in

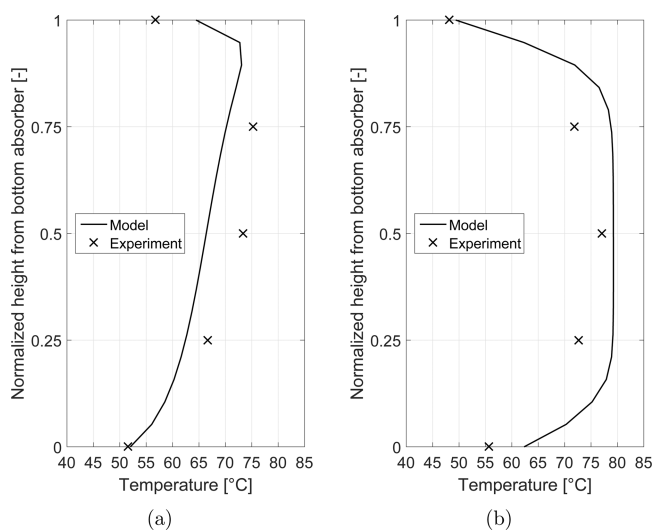


Figure 6. Absorber temperature profile: comparison of experimental data and model results referring to the open-loop step response test with increasing flue gas flow rate. Absorber temperature profile (a) before and (b) 120 min after the perturbation.

flue gas flow (Figure 5a) results in an increase of the L/G ratio in the absorber and therefore in an increase of the CO₂ capture rate (Figure 5b). However, a lower amount of CO₂ is captured,

which is primarily absorbed by the solvent in the lower part of the absorber column. As a consequence, the temperature at the absorber bottom and in the sump increases, and the temperature at the column top decreases. Figure 5c presents the comparison of the model predictions and measurements for the response in the absorber temperatures. The simulation results show the same trend as the measurements. Considering rise and settling time of the transient, the predictions of the absorber bottom and top temperature compare well with the experimental data. However, for the sump temperature, the model predicts a gradual change starting at $t = 0$ min, while during the experiment, the sump temperature increases only after 15 min and then rather rapidly. This mismatch might be explained by the fact that perfect mixing is assumed in the sump model, which might not be the case during the experiment.

With respect to the steady-state absorber temperature values, the model does not accurately predict the initial and final values, with differences up to 7 °C. This might be attributed to an inaccurate estimation of the heat of absorption and heat of reaction, or the solubility, thus resulting in an inaccurate prediction of the heat distribution throughout the absorber column, as shown in Figure 6. Another explanation for the deviations is the use of equilibrium stages instead of a rate-based modeling approach. In general, the model underestimates the temperature profile during initial steady-state and overestimates the profile at the final off-design operating point. The accuracy of the absorber model predictions might be improved by using a rate-based model. However, it is known³⁹ that the accuracy obtained with the equilibrium-based model is

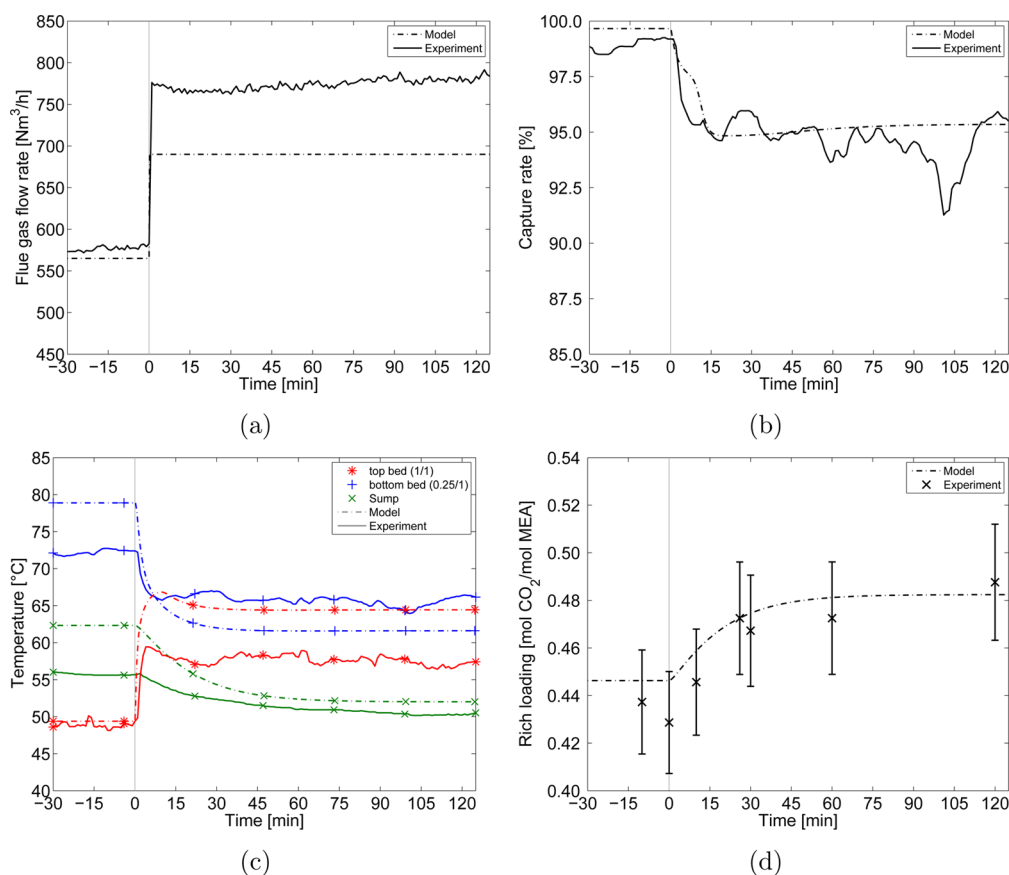


Figure 7. Comparison of experimental data (solid line) and model results (dashed line) for open-loop step response test: increase in flue gas flow rate. (a) Flue gas flow rate, (b) capture rate, (c) absorber column temperatures, and (d) rich solvent loading.

sufficient for dynamic system simulations aimed at control design studies, whereby the interest is more on the correct estimation of the transient than on the absorber temperature values.

Figure 5d depicts the comparison between model predictions and experimental values in terms of rich loading. The rich loading decreases due to the decrease in flue gas flow rate. The transient of the loading is correctly predicted by the model. As far as the final steady-state is concerned, the model slightly overpredicts the rich loading, but the values are well within the measurement accuracy. Finally, it is worth pointing out the periodic fluctuations of the capture rate at time -20 , 20 , 60 , and 100 min. The temporary decrease in capture rate is caused by an unstable operation of the steam generator, which is however not included in the capture plant model.

Figure 7 shows the comparison of model predictions and experimental data for test A2, during which an inverse step of the same magnitude was applied to the flue gas flow rate (Figure 7a). A similar but reverse response with respect to test A1 is expected as the perturbations are small. Because of the increase in flue gas flow rate, the capture rate (Figure 7b) decreases, the temperature at the absorber top increases, and the temperatures at the lower part of the absorber including the sump decrease (Figure 7c). Good agreement is achieved for the rise and settling time of the temperature transients. In comparison to test A1, the measured transient of the sump temperature is different. It seems that during this experiment the mixing in the sump was much better leading to the gradual temperature decrease, which is also predicted by the model. As far as steady-state values are concerned, the deviations in the absorber temperature profile are likely attributed to the assumption of thermodynamic equilibrium in the absorber model. Figure 7d visualizes the measurements and model prediction for the transient of the rich loading. The model predictions show good agreement with the experimental data in terms of the transient time. The settling time of the rich loading is also in line with the total solvent residence time of 52 min. The off-design steady-state values are slightly overpredicted but well within the error bars indicating the accuracy of the measurement method.

As highlighted during the discussion of test A1 results, the fluctuations in the capture rate were primarily caused by unstable operation of the steam generator.

Partially comparable simulation and experimental studies were carried out by Zhang et al. and Bui et al.^{40,41} Their findings confirm, in a qualitative manner, the observation of a strong interaction between the flue gas flow and the capture rate. Furthermore, the time constants of the capture rates reported in Zhang et al. and Bui et al. are similar to those documented here.

5. CASE STUDY

Ramp rates for load variation of conventional coal-fired power plants are limited by the ramping speed capabilities of the furnace, which, for modern power plants, are typically in the range of 1–5% per minute of the nominal power output.^{42,43} Higher ramp rates can be achieved for systems with an integrated PCC plant by adjusting the steam extraction flow to the reboiler of the capture system instead of changing the furnace load. In this case, the limiting factor is the valve stroke time. Common valve stroke times are in the range of 10–900 s. Here, a stroke time of 30 s was chosen as a ramp rate for the steam extraction.⁴⁴ Such an operating scenario offers the

possibility to respond faster to rapid changes in electricity demand or to react to situations in which it is economically more favorable to generate electricity instead of capturing CO₂. In the case described here, an increase of 5% of the nominal power output is assumed. The required steam extraction and subsequent reboiler duty reduction to achieve this power increase were estimated using the power loss correlations developed by Linnenberg et al.⁴⁵ These correlations assume a tapping steam pressure of 3.9 bar for a hard-coal fired power plant with a nominal net power output of 1015 MW_{el}. By setting the tapping steam pressure to a constant value, off-design turbine operation is excluded from this study. An increase in net power output by 5% requires a reduction of the reboiler duty by 25% (see Table 8). The capture plant model is at pilot scale; thus, the same relative changes were used because the reboiler duty scales proportionally to the size of the plant.

Table 8. Power Loss and Steam Extraction Calculation Results To Determine the Required Reduction of Reboiler Duty for an Increase of Net Power Output

variable	unit	without capture	with capture (nominal load)	with capture (decreased reboiler duty)
heat input	MW _{th}	2232	2232	2232
gross power output	MW _{el}	1100	1100	1100
steam extraction	MW _{th}	0	672	500
net power output	MW _{el}	1015	861	904

Two cases were simulated to assess the transient performance of the capture plant during a reduction of the reboiler duty by 25% within 30 s, followed by an inverse increase of the same magnitude. For both simulations, the tuned pilot plant model was used, in which an additional controller for maintaining the L/G ratio was implemented.

In the first case (case A), all controller set points of the capture plant remained unchanged during the decrease of reboiler duty. This led to a lower reboiler temperature. Thus, the lean loading increases resulted in a decrease of the capture rate. In the second case (case B), next to the reboiler duty also the flue gas flow was decreased by 25% to maintain a more stable operation and constant capture rate. This reduction can be achieved by partially bypassing the flue gas sent to the capture plant and venting it directly to the chimney.

Figures 8 and 9 show the comparison of the simulation results for cases A and B in terms of the main process variables, whereby the results of case A are displayed on the left side of both figures and the results of case B on the right. The downward step is applied at $t = 0$ min and the upward step at $t = 120$ min, such that steady-state conditions are obtained after the first perturbation.

Considering the response in case A, the reduction of reboiler duty (downward step) results in a decrease of the reboiler temperature by 1.9 °C (Figure 8e). Because of the lower temperature level, less CO₂ is desorbed within the stripper column leading a gradual increase of the lean loading (Figure 9a). Because of the increasing loading of the lean solvent, less CO₂ is removed from the flue gas in the absorber column, which subsequently results in a decrease of the absorber temperatures. In Figure 9c, it can be observed that the change in absorber temperature profile starts with a delay of few

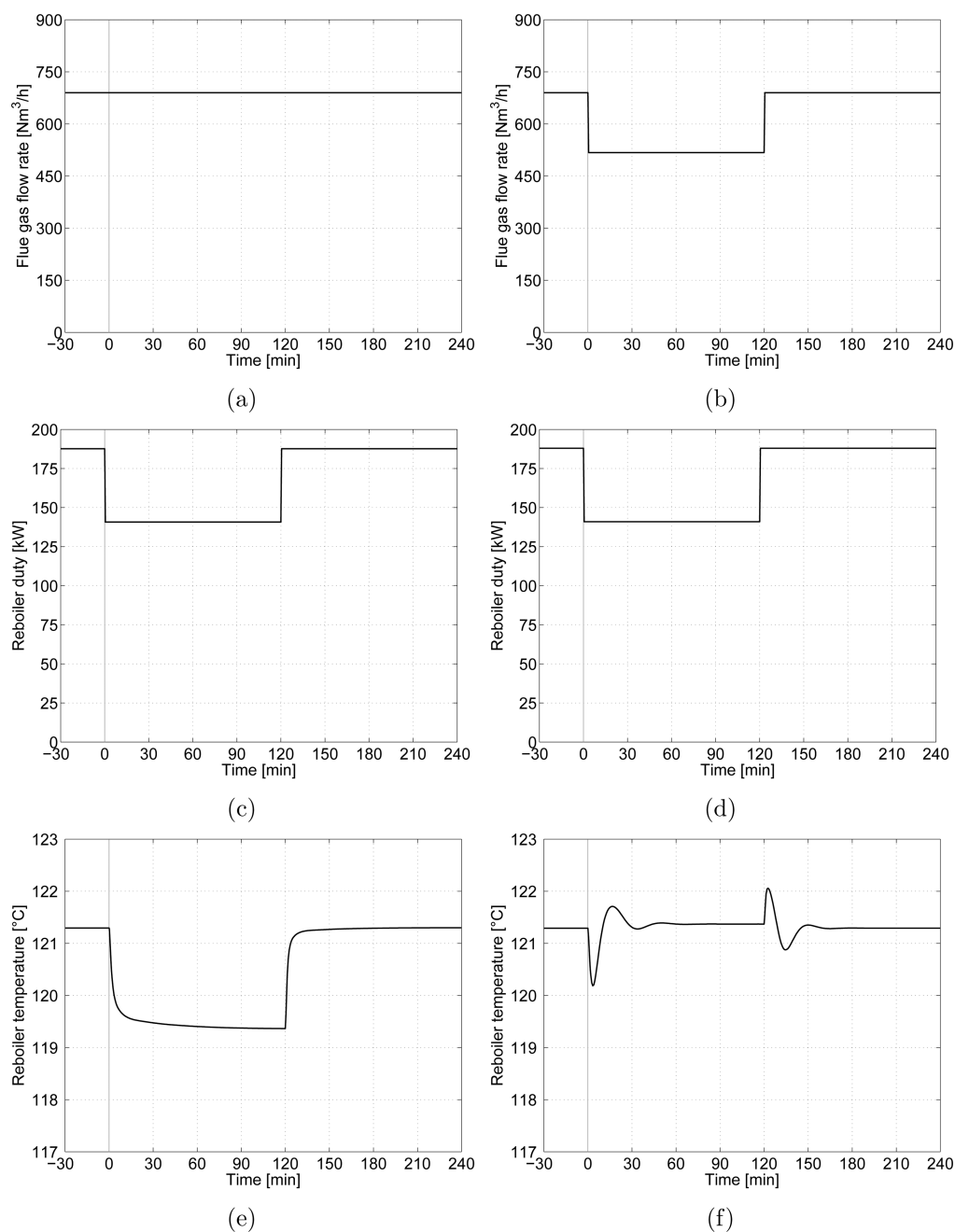


Figure 8. Comparison of simulation results of the flue gas flow, reboiler duty, and reboiler temperature for case A (left) and case B (right).

minutes with respect to the initial perturbation. At the top of the absorber, the temperature difference between initial and final steady-state is the largest, 6.2 K. The rich loading is almost unaffected by the changes (Figure 8a), and the capture rate decreases given that the flue gas flow is maintained (Figure 9e). Considering all displayed variables, within 60 min, the final steady-state values are reached within $\pm 1\%$ difference. The subsequent upward step at $t = 120$ min leads to an inverse response returning to the initial on-design operating point. Tait et al.⁴⁶ performed a similar experimental scenario using a pilot capture plant. The steam flow to the reboiler was rapidly decreased, while the flue gas flow to the absorber was maintained. Lawal et al.⁴⁷ simulated a rapid reduction of the reboiler duty with a similar capture plant model. In both studies, it was observed that the applied perturbation led to

strong disturbances of the capture process and that the solvent inventories had a significant effect on the settling time.

With respect to simulation of case B, the capture system transient is a combination of the response to the change in reboiler duty and to the simultaneous adjustment of the flue gas flow. Hence, the initial response on the stripper side is similar to case A. The reboiler temperature decreases due to the reduction in reboiler duty (Figure 8f). However, on the absorber side, the initial response is determined by the reduction in flue gas flow rate (Figure 8b). Because of the fast decrease in flue gas, in total less CO_2 is absorbed by the solvent in the absorber column, which leads to initially rapid changes in the temperature profile, in particular in the first bed (Figure 9d). Then the L/G controller reacts on the changes in flue gas by reducing the solvent flow rate, and consequently the absorber temperatures return to their initial values after slight

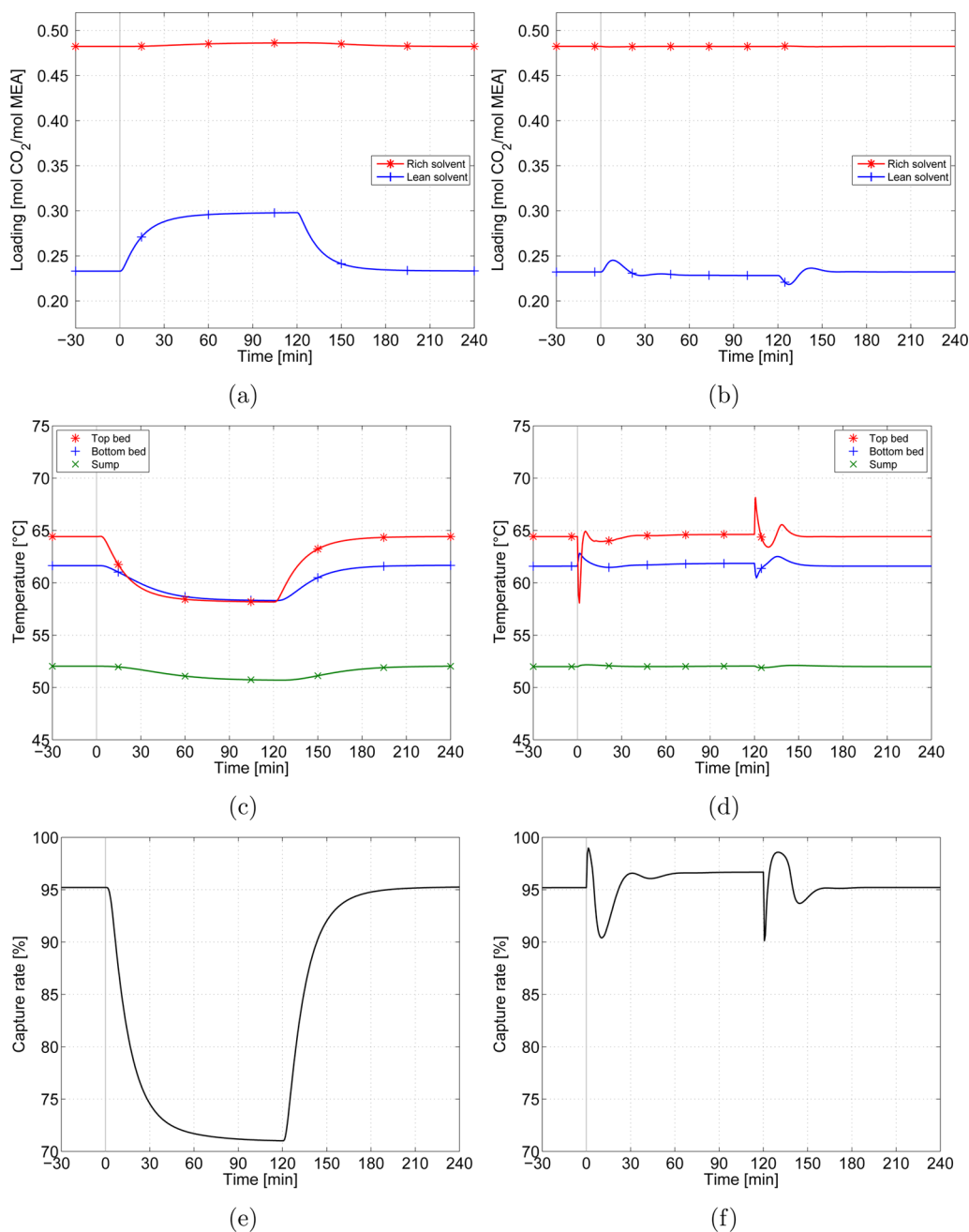


Figure 9. Comparison of simulation results of the rich and lean solvent loading, absorber temperatures, and the capture rate for case A (left) and case B (right).

fluctuations caused by the changes in the stripper. After a few minutes, the reboiler temperature increases again, due to the lower solvent flow which needs to be regenerated, and reaches approximately its initial value after a slight overshoot. A small temporary increase is observed in the lean loading, while the rich loading is unaffected (Figure 9b). The capture rate displays fluctuations, but its value is approximately maintained due to the simultaneous decrease of reboiler duty and flue gas flow. The subsequent downward step results in a similar but inverse response. The simulations of case B show that the new steady-state values are reached within $\pm 1\%$ after approximately 30 min. Enaasen Flø et al.⁴⁸ simulated a similar operating condition in which the flue gas is partly vented by reducing the flue gas flow rate to the absorber by 24%. The solvent flow rate and steam flow rate to the reboiler have been decreased

proportionally to the flue gas flow rate, similarly to case B as presented here. The solvent flow rate and steam flow to the reboiler have been increased during a period of normal electricity prices to keep a time average capture rate of 90%. The response of the solvent loading observed by Enaasen Flø et al. is similar to the one documented here, but it shows larger fluctuations, probably caused by the larger magnitude of the perturbation.

The simulations of case A and B allow researchers to state that both operations are feasible and safe. Further, it can be observed that the settling time for case A is higher than for case B (60 versus 30 min to reach the new steady-state within $\pm 1\%$ difference). This assessment is important as it determines how fast the plant can return to the initial capture target once the steam tapping valve is opened again.

A disadvantage of scenario A is that the absorber and stripper are operated at off-design in terms of temperatures and solvent loading after the reduction in reboiler duty. In case of scenario B, the temperatures in both columns are maintained after the perturbation by operating at lower flow rates. Thus, the energy efficiency is higher for case B than for case A.

It shall also be remarked that the transient of case A is very smooth for all variables, whereas in case B, fluctuations are observed in some variables due to the simultaneous perturbation of reboiler duty and flue gas flow based on constant ramp rates. Ultimately, the aim should be to design a control system which adjusts the flue gas and solvent flow such that in particular the temperature transient in the absorber and stripper are smooth. As a result, the fluctuations observed in case B could be further reduced.

6. CONCLUSION AND RECOMMENDATION

This paper presents a dynamic modeling, validation, and a transient operation study related to an amine-based PCC plant. The model was developed using the open source Thermal-Separation Modelica library and validated against experimental data obtained from the capture pilot plant at the Maasvlakte power station in the Netherlands.

The settling time of the pilot plant was approximately 50 min, and the experiments as well as the model simulations showed that this is strongly influenced by the liquid hold-up throughout the plant's sumps and tanks. Consequently, if a scale-up of the plant is considered, these volumes are an extremely relevant design parameter, especially in case requirements on flexible operation are stringent. In addition, large-scale capture plants should be equipped with advanced control systems^{49,50} to enable the plant to promptly respond to load variations and minimize the time to return to steady-state operating conditions. In case this technology will be applied and if future operating conditions will demand for frequent and large load changes, it might be that the time needed for a capture plant to reach steady state will considerably increase.

Furthermore, the work documented in this publication demonstrates that the tuned equilibrium-based model for chemical absorption of CO₂ provides sufficiently accurate transient performance predictions for the purpose of dynamic process analysis. This conclusion is supported by the good agreement between experimental data and simulation results for transient operation ensuing from a rapid perturbation of the flue gas flow. Larger deviations are observed for steady-state predictions of the absorber temperature profile, which might be improved by adopting a rate-based model. However, for the transient analysis of the entire system formed by the power plant and the capture unit, a rate-based model is less suitable due to the increase in model complexity that leads to higher computational effort.

The validated capture plant model was subsequently used to assess the impact of transient power plant operation on power plant and capture plant performance. It was demonstrated that fast load variations in terms of reboiler duty and flue gas flow constitute a feasible operating mode for the capture unit. This enables the fossil-fuelled power plant to respond faster to changes in the electricity demand by reducing the steam extraction flow to the reboiler of the capture system instead of adjusting the furnace load.

In a following research phase, the model of the power plant and of the capture unit should be integrated into a single model. The flexibility of the object-oriented modeling easily

enables such integration thanks to the possibility of extending existing models. The ultimate aim is to use the integrated system model for a complete analysis of transient operation and the design of control strategies as well as the tuning of control parameters to improve dynamic performance.

■ ASSOCIATED CONTENT

📄 Supporting Information

The Supporting Information is available free of charge on the ACS Publications website at DOI: [10.1021/acs.iecr.6b00034](https://doi.org/10.1021/acs.iecr.6b00034).

Data from experiments Test A1, A2, and B1 (PDF)

■ AUTHOR INFORMATION

Corresponding Author

*E-mail: P.Colonna@TUDelft.nl.

ORCID

Adam van de Haar: 0000-0002-7512-7554

Notes

The authors declare no competing financial interest.

■ ACKNOWLEDGMENTS

The work described in this article has been developed as a close collaboration of TU Hamburg-Harburg, TU Delft, and TNO. The experiments to obtain pilot plant data were sponsored by the CATO2 program. The authors gratefully acknowledge the contribution of all involved parties.

■ REFERENCES

- (1) Bui, A.; Gunawan, I.; Verheyen, V.; Feron, P.; Meuleman, E.; Adeloju, S. Dynamic modelling and optimization of flexible operation in post-combustion CO₂ capture plants-A review. *Comput. Chem. Eng.* **2014**, *61*, 245–265.
- (2) Puxty, G.; Rowland, R.; Allport, A.; Yang, Q.; Bown, M.; Burns, R.; Maeder, M.; Attalla, M. Carbon Dioxide Postcombustion Capture: A Novel Screening Study of the Carbon Dioxide Absorption Performance of 76 Amines. *Environ. Sci. Technol.* **2009**, *43* (16), 6427–6433.
- (3) McKetta, J. *Encyclopedia of Chemical Processing and Design*; CRC Press, 1978; Vol. 6, pp 292–301.
- (4) Mac Dowell, N.; Staffell, I. The role of flexible CCS in the UK's future energy system. *Int. J. Greenhouse Gas Control* **2016**, *48*, 327–344.
- (5) Patino-Echeverri, D.; Hoppock, D. C. Reducing the average cost of CO₂ capture by shutting-down the capture plant at times of high electricity prices. *Int. J. Greenhouse Gas Control* **2012**, *9*, 410–418.
- (6) Cohen, S. M.; Rochelle, G. T.; Webber, M. E. Optimizing post-combustion CO₂ capture in response to volatile electricity prices. *Int. J. Greenhouse Gas Control* **2012**, *8*, 180–195.
- (7) Zaman, M.; Lee, J. H. Optimization of the various modes of flexible operation for post-combustion CO₂ capture plant. *Comput. Chem. Eng.* **2015**, *75*, 14–27.
- (8) Ho, M. T.; Wiley, D. E. Flexible strategies to facilitate carbon capture deployment at pulverised coal power plants. *Int. J. Greenhouse Gas Control* **2016**, *48*, 290–299.
- (9) van der Wijk, P.; Brouwer, A.; van den Broek, M.; Slot, T.; Stienstra, G.; van der Veen, W.; Faaij, A. Benefits of coal-fired power generation with flexible CCS in a future northwest European power system with large scale wind power. *Int. J. Greenhouse Gas Control* **2014**, *28*, 216–233.
- (10) Brunnemann, J.; Gottelt, F.; Wellner, K.; Renz, A.; Thüning, A.; Roeder, V.; Hasenbein, C.; Schmitz, G.; Eiden, J. Status of ClaRaCCS: Modelling and Simulation of Coal-Fired Power Plants with CO₂ Capture. *Proceedings of the 9th International Modelica Conference 2012*, 609–618, DOI: [10.3384/epc12076609](https://doi.org/10.3384/epc12076609).

- (11) Ziaii, S. *Dynamic Modeling, Optimization, and Control of Monoethanolamine Scrubbing for CO₂ Capture*. Dissertation, University of Texas at Austin, 2012.
- (12) Harun, N.; Nittaya, T.; Douglas, P. L.; Croiset, E.; Ricardez-Sandoval, L. A. Dynamic simulation of MEA absorption process for CO₂ capture from power plants. *Int. J. Greenhouse Gas Control* **2012**, *10*, 295–309.
- (13) Jayarathna, S. A.; Lie, B.; Melaen, M. C. Dynamic modelling of the absorber of a post combustion CO₂ capture plant: modelling and simulations. *Comput. Chem. Eng.* **2013**, *53*, 178.
- (14) Kvamsdal, H. M.; Chikukwa, A.; Hillestad, M.; Zakeri, A.; Einbu, A. A comparison of different parameter correlation models and the validation of an MEA-based absorber model. *Energy Procedia* **2011**, *4*, 1526–1533.
- (15) Lawal, A.; Wang, M.; Stephenson, P.; Yeung, H. Dynamic modelling of CO₂ absorption for post combustion capture in coal-fired power plants. *Fuel* **2009**, *88*, 2455–2462.
- (16) Ceccarelli, N.; van Leeuwen, M.; Wolf, T.; van Leeuwen, P.; van der Vaart, R.; Maas, W.; Ramos, A. Flexibility of low-CO₂ gas power plants: Integration of the CO₂ capture unit with CCGT operation. *Energy Procedia* **2014**, *63*, 1703–1726.
- (17) Posch, S.; Haider, M. Dynamic modeling of CO₂ absorption from coal-fired power plants into an aqueous monoethanolamine solution. *Chem. Eng. Res. Des.* **2013**, *91*, 977–987.
- (18) Åkesson, J.; Faber, R.; Laird, C.; Prölb, K.; Tummeseit, H.; Velut, S.; Zhu, Y. Models of a post-combustion absorption unit for simulation, optimization and non-linear model predictive control schemes. *8th International Modelica Conference*, 2011.
- (19) Faber, R.; Köpcke, M.; Biede, O.; Knudsen, J. N.; Andersen, J. Open-loop step responses for the MEA post-combustion capture process: Experimental results from the Esbjerg pilot plant. *Energy Procedia* **2011**, *4*, 1427–1434.
- (20) Enaasen Flø, N.; Knuutila, H.; Kvamsdal, H. M.; Hillestad, M. Dynamic model validation of the post-combustion CO₂ absorption process. *Int. J. Greenhouse Gas Control* **2015**, *41*, 127–141.
- (21) Biliyok, C.; Lawal, A.; Wang, M.; Seibert, F. Dynamic modelling, validation and analysis of post-combustion chemical absorption CO₂ capture plant. *Int. J. Greenhouse Gas Control* **2012**, *9*, 428–445.
- (22) Walters, M.; Lin, Y.; Sachde, D.; Edgar, T.; Rochelle, G. Control Relevant Model of Amine Scrubbing for CO₂ Capture from Power Plants. *Ind. Eng. Chem. Res.* **2016**, *55*, 1690–1700.
- (23) Modelica, Version 3.3; Modelica Association, 2014. <http://www.modelica.org> (accessed January 2016).
- (24) Dietl, K. *Equation-Based Object-Oriented Modelling of Dynamic Absorption and Rectification Processes*. Dissertation, Hamburg University of Technology, Institute of Thermo-Fluid Dynamics, 2012.
- (25) Testing Post Combustion Capture. *Carbon Capture J.* **2008**, *5*, 10.
- (26) Oexmann, J. *Post-Combustion CO₂ Capture: Energetic Evaluation of Chemical Absorption Processes in Coal-Fired Steam Power Plants*. Dissertation, University Hamburg-Harburg, Institute of Energy Systems, Hamburg, 2011.
- (27) Hilliard, M. *A Predictive Thermodynamic Model for an Aqueous Blend of Potassium Carbonate, Piperazine, and Monoethanolamine for Carbon Dioxide Capture from Flue Gas*. Dissertation, University of Texas at Austin, 2008.
- (28) Davis, J.; Rochelle, G. Thermal degradation of monoethanolamine at stripper conditions. *Energy Procedia* **2009**, *1*, 327–333.
- (29) Casella, F.; Leva, A. Modelling of Thermo-Hydraulic Power Generation Processes Using Modelica. *Math. Comput. Model. Dyn. Syst.* **2006**, *12* (1), 19–33.
- (30) Casella, F.; Leva, A. Object-oriented modelling & simulation of power plants with Modelica. *Proceedings of the 44th IEEE Conference on Decision and Control, and the European Control Conference, CDC-ECC '05*; IEEE, 2005; pp 7597–7602.
- (31) Dietl, K.; Joos, A.; Schmitz, G. Dynamic analysis of the absorption/desorption loop of a carbon capture plant using an object-oriented approach. *Chem. Eng. Process.* **2012**, *52*, 132–139.
- (32) Wellner, K.; Trapp, C.; Schmitz, G.; Casella, F. Interfacing Models for Thermal Separation Processes with Fluid Property Data from External Sources. *Proceedings 10th Modelica Conference*, Lund, Sweden, March 10–12, 2014.
- (33) Trapp, C.; Casella, F.; van der Stelt, T. P.; Colonna, P. Use of External Fluid Property Code in Modelica for Modelling of a Precombustion CO₂ Capture Process Involving Multicomponent, Two-Phase Fluids. *Proceedings 10th Modelica Conference*, Lund, Sweden, March 10–12, 2014.
- (34) Kenig, E.; Schneider, R.; Górak, A. Reactive absorption: Optimal process design via optimal modelling. *Chem. Eng. Sci.* **2001**, *56*, 343–350.
- (35) Jou, F.; Mather, A.; Otto, F. The Solubility of CO₂ in a 30 Mass Percent Monoethanolamine Solution. *Can. J. Chem. Eng.* **1995**, *73*, 140–147.
- (36) Dugas, R. *Carbon Dioxide Absorption, Desorption, and Diffusion in Aqueous Piperazine and Monoethanolamine*. Dissertation, University of Texas at Austin, 2009.
- (37) Stichlmair, J.; Bravo, J.; Fair, J. General model for prediction of pressure drop and capacity of countercurrent gas/liquid packed columns. *Gas Sep. Purif.* **1989**, *3*, 19–28.
- (38) van de Haar, A. M. *Analysis of the Dynamic Performance of a MEA-Based Carbon Capture Unit for Coal-Fired Power Plants*. Master's Thesis, Delft University of Technology, 2013.
- (39) Krishnamurthy, R.; Taylor, R. A nonequilibrium stage model of multicomponent separation processes. Part III: The Influence of Unequal Component-Efficiencies in Process Design Problems. *AIChE J.* **1985**, *31*, 1973–1985.
- (40) Zhang, Q.; Turton, R.; Bhattacharyya, D. Development of Model and Model-Predictive Control of an MEABased Postcombustion CO₂ Capture Process. *Ind. Eng. Chem. Res.* **2016**, *55*, 1292–1308.
- (41) Bui, A.; Gunawan, I.; Verheyen, V.; Feron, P.; Meuleman, E. Flexible operation of CSIRO's post-combustion CO₂ capture pilot plant at the AGL Loy Yang power station. *Int. J. Greenhouse Gas Control* **2016**, *48*, 188–203.
- (42) Ziems, C.; Weber, H.; Meinke, S.; Hassel, E.; Jürgen, N. Ratio between conventional and renewable energy production in Germany with focus on 2020. *VGB PowerTech* **2011**, *8*, 35–42.
- (43) Lindsay, J.; Dragoon, K. *Summary Report on Coal Plant Dynamic Performance Capability*; Renewable Northwest, 2010.
- (44) Schulze, S. *Continuous Modulating Actuators Improve Plant Efficiency*; Power Engineering, 2012. <http://www.power-eng.com/articles/print/volume-116/issue-8/features/continuous-modulating-actuators.html> (accessed June 14, 2014).
- (45) Linnenberg, S.; Liebenthal, U.; Oexmann, J.; Kather, A. Derivation of power loss factors to evaluate the impact of postcombustion CO₂ capture processes on steam power plant performance. *Energy Procedia* **2011**, *4*, 1385–1394.
- (46) Tait, P.; Buschle, B.; Ausner, I.; Valluri, P.; Wehrli, M.; Lucquiaud, M. A pilot-scale study of dynamic response scenarios for the flexible operation of post-combustion CO₂ capture. *Int. J. Greenhouse Gas Control* **2016**, *48*, 216–233.
- (47) Lawal, A.; Wang, M.; Stephenson, P.; Koumpouras, G.; Yeung, H. Dynamic modelling and analysis of post-combustion CO₂ chemical absorption process for coal-fired power plants. *Fuel* **2010**, *89*, 2791–2801.
- (48) Flø, N. E.; Kvamsdal, H. M.; Hillestad, M. Dynamic simulation of post-combustion CO₂ capture for flexible operation of the Brindisi pilot plant. *Int. J. Greenhouse Gas Control* **2016**, *48*, 204–215.
- (49) Hossein Sahraei, M.; Ricardez-Sandoval, L. Controllability and optimal scheduling of a CO₂ capture plant using model predictive control. *Int. J. Greenhouse Gas Control* **2014**, *30*, 58–71.
- (50) Walters, M. S.; Edgar, T. F.; Rochelle, G. T. Regulatory Control of Amine Scrubbing for CO₂ Capture from Power Plants. *Ind. Eng. Chem. Res.* **2016**, *55*, 4646–4657.